

# A Highly Fatigue-Resistant Zr-Based Bulk Metallic Glass

STEVEN E. NALEWAY, RAWLEY B. GREENE, BERND GLUDOVATZ,  
NEIL K.N. DAVE, ROBERT O. RITCHIE, and JAMIE J. KRUZIC

The strength-normalized fatigue endurance strength of the bulk metallic glass (BMG)  $Zr_{52.5}Cu_{17.9}Ni_{14.6}Al_{10}Ti_5$  (Vitreloy 105) has been reported to be the highest for any BMG; however, to date, there has been no explanation of why this material is so much better than other Zr-based compositions. In this study, the fatigue-crack growth behavior of  $Zr_{52.5}Cu_{17.9}Ni_{14.6}Al_{10}Ti_5$  was compared in ambient air vs dry nitrogen environment. The excellent fatigue life behavior is attributed to a relatively high fatigue threshold ( $\Delta K_{TH} \approx 2 \text{ MPa}\sqrt{\text{m}}$ ) and a lack of sensitivity to environmental effects on fatigue-crack growth in ambient air, as compared to other Zr-based BMGs. Fatigue life experiments conducted in ambient air confirmed the excellent fatigue life properties with a  $10^7$ -cycle endurance strength of  $\sim 0.24$  of the ultimate tensile strength; however, it was also found that casting porosity, even in limited amounts, could reduce this endurance strength by as much as  $\sim 60$  pct. Overall, the BMG  $Zr_{52.5}Cu_{17.9}Ni_{14.6}Al_{10}Ti_5$  appears to have excellent strength and fatigue properties and should be considered as a prime candidate material for future applications where good mechanical fatigue resistance is required.

DOI: 10.1007/s11661-013-1923-4

© The Minerals, Metals & Materials Society and ASM International 2013

## I. INTRODUCTION

BULK metallic glasses (BMGs) are a relatively new class of engineering materials with unique properties that make them potential candidates for many structural applications.<sup>[1]</sup> Favorable properties include near-theoretical strengths combined with reasonably high fracture toughness, low damping, large elastic strain limits, and the ability to be thermoplastically formed into precision-shaped parts with complex geometries,<sup>[2,3]</sup> all properties that are generally distinct from, or superior to, corresponding crystalline metals and alloys. One property which has been perceived as a limitation for BMGs has been low fatigue resistance relative to crystalline metallic materials; indeed, the first study on  $Zr_{41.25}Ti_{13.75}Ni_{10}Cu_{12.5}Be_{22.5}$  (Vitreloy 1),\* the most studied BMG, found

the endurance strength to be only  $\sim 4$  pct of the ultimate tensile strength ( $\sigma_{fat}/\sigma_{UTS} \approx 0.04$ ) in four-point bending at a load ratio of minimum to maximum load of  $R = P_{min}/P_{max} = 0.1$ .<sup>[4]</sup> At the time, such poor fatigue performance was attributed to the lack of microstructure in monolithic glasses which could arrest incipient flaws; however, more recently, a monolithic Zr-based BMG, Vitreloy 105, with composition  $Zr_{52.5}Cu_{17.9}Ni_{14.6}Al_{10}Ti_5$ , has been reported to have excellent fatigue resistance, specifically a  $10^7$ -cycle endurance strength of  $\sigma_{fat}/\sigma_{UTS} \approx 0.25$  (in four-point bending at  $R = 0.1$ ), which is better than, or comparable to, all other monolithic glasses and indeed even many crystalline metals.<sup>[5,6]</sup> Since neither of these monolithic BMGs has microstructure, other factors must govern the large difference in fatigue resistance.

Recently, it has been shown that there is a significant environmental degradation of fatigue properties for Zr-Ti-Cu-Ni-Be BMGs in ambient air which causes a low fatigue threshold and a stress intensity-independent regime of fatigue-crack growth.<sup>[7]</sup> Furthermore, it has been suggested that the environmental degradation may be the dominant factor explaining the low measured endurance limit for Zr-Ti-Cu-Ni-Be BMGs.<sup>[8]</sup> Accordingly, the purpose of this paper is to test the hypothesis that the characteristic low fatigue thresholds and stress intensity-independent growth regimes seen in Zr-Ti-Cu-Ni-Be and Zr-Cu-Ni-Al-Nb BMG compositions<sup>[7,9-11]</sup> are absent for Vitreloy 105 and may be associated with the high reported fatigue endurance strength. Additionally, the role of casting porosity in reducing these fatigue properties is also examined as this may have played a role in some of the early reports of very poor fatigue behavior in other Zr-based BMGs.

---

\*All compositions are given in terms of atomic percent.

---

STEVEN E. NALEWAY and RAWLEY B. GREENE, Graduate Research Assistants, and JAMIE J. KRUZIC, Associate Professor, are with the Materials Science Program, School of Mechanical, Industrial, and Manufacturing Engineering, Oregon State University, Corvallis, OR 97331. Contact e-mail: jamie.kruzic@oregonstate.edu BERND GLUDOVATZ, Postdoctoral Fellow, is with the Materials Sciences Division, Lawrence Berkeley National Laboratory, Berkeley, CA 94720. NEIL K.N. DAVE, Graduate Research Assistant, and ROBERT O. RITCHIE, Professor, are with the Materials Sciences Division, Lawrence Berkeley National Laboratory, and also with the Department of Materials Science and Engineering, University of California, Berkeley, CA 94720.

Manuscript submitted February 8, 2013.

Article published online August 13, 2013

## II. MATERIALS AND METHODS

### A. Materials

Research grade  $Zr_{52.5}Cu_{17.9}Ni_{14.6}Al_{10}Ti_5$  BMG plates nominally  $30 \times 30 \text{ mm}^2$  were procured from Liquidmetal Technologies (Rancho Santa Margarita, CA). Fully amorphous cast plates were machined into compact tension C(T) samples (width,  $W = 21.5 \text{ mm}$ , thickness,  $B = 2.0 \text{ mm}$ ) in accordance with the ASTM standard E647 for fatigue-crack growth studies.<sup>[12]</sup> The faces of each sample were subsequently polished to a  $0.05 \mu\text{m}$  finish to facilitate accurate crack length measurements using optical microscopy. The samples were annealed at  $573 \text{ K}$  ( $300 \text{ }^\circ\text{C}$ ) for 2 minutes in flowing ultrahigh purity nitrogen to relieve surface stresses incurred by thermal tempering during casting, which are known to affect the fatigue behavior of Zr-based BMGs.<sup>[10]</sup> This temperature is well below the glass transition temperature ( $T_g \sim 682 \text{ K}$  to  $713 \text{ K}$  ( $409 \text{ }^\circ\text{C}$  to  $440 \text{ }^\circ\text{C}$ )<sup>[13]</sup>) noting that the exact value of  $T_g$  depends on various factors including impurity content, the rate at which the supercooled liquid is cooled through the glass transition, and the rate which it is reheated from its glassy state back into the supercooled liquid. The fully amorphous nature of the plates was confirmed using X-ray diffraction (XRD) before and after annealing, as shown in Figure 1.

Beams used for fatigue life tests were machined from the same plates described above, specifically from regions of the fractured C(T) specimens far from the crack growth. The fatigue life samples had a thickness  $B$ , width  $W$ , and length  $L$  of  $\sim 2 \times 2 \times 25 \text{ mm}^3$ , respectively, and were first ground gradually with 180# to 4000# silicon carbide paper before being polished with diamond paste to a  $1 \mu\text{m}$  finish on the tensile surface; the corners next to the tensile surface were slightly rounded to reduce the stress concentration. A few samples contained large casting pores exceeding  $\sim 10 \mu\text{m}$  in diameter. Since identifying such samples was impossible before testing, the after testing fracture surfaces were examined instead in a scanning electron microscope and samples that had failure initiating at large

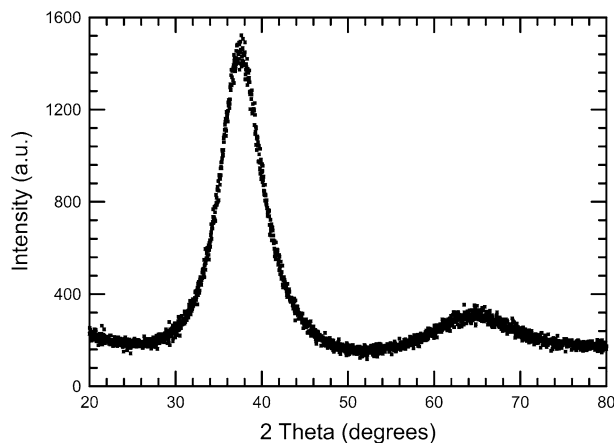


Fig. 1—X-ray diffraction scan performed at 0.75 deg per minute showing the fully amorphous nature of the  $Zr_{52.5}Cu_{17.9}Ni_{14.6}Al_{10}Ti_5$  BMG.

casting pores were placed in a separate group from defect-free samples.

### B. Fatigue Experiments

Fatigue life tests were performed in four-point bending (tension–tension loading) using an inner loading span  $S_1 = 10 \text{ mm}$  and an outer span  $S_2 = 20 \text{ mm}$ , such that  $S_1 > 2W$  and  $S_2 > 4W$ . Samples were tested in ambient air under load control at a frequency of 25 Hz (sine wave) with a constant load ratio of  $R = 0.1$  using a servo-hydraulic MTS 810 mechanical testing machine (MTS Corporation, Eden Prairie, MN). The maximum tensile stresses  $\sigma$  within the inner span were calculated using simple beam mechanics theory:

$$\sigma = \frac{3P(S_2 - S_1)}{2BW^2}, \quad [1]$$

where  $P$  is the applied load. Beams were tested at a normalized stress amplitude\*\* from  $\sigma_a/\sigma_{UTS} \approx 0.22$  to

---

\*\*The stress amplitude,  $\sigma_a$ , is half of the stress range,  $\Delta\sigma = \sigma_{\min} - \sigma_{\max}$ , where  $\sigma_{\min}$  and  $\sigma_{\max}$  correspond to the minimum and maximum values of the applied stress.

---

0.38; tests were terminated in cases where failure had not occurred after  $2 \times 10^7$  cycles. The value of  $\sigma_{UTS} = 1700 \text{ MPa}$  was taken from Reference 5.

Fatigue-crack growth tests were performed in ambient air and dry gaseous nitrogen environments using a computer-controlled servo-hydraulic Instron 8501 mechanical testing machine (Instron Corporation, Norwood, MA) at a constant frequency of 25 Hz (sine wave) with a constant ratio of  $R = 0.1$ . The nominal test temperature was  $23 \pm 2 \text{ }^\circ\text{C}$  and the air relative humidity was in the range of 20 to 40 pct. To obtain the fatigue-crack growth curve in an inert environment, two samples were tested in an aluminum and stainless steel test chamber in flowing dry  $N_2$  gas which had been passed through a purifier (Gatekeeper, Aeronex, San Diego, CA) rated to achieve sub-parts per billion (ppb) levels of oxygen and moisture. Before testing, a bake-out procedure was performed to remove contaminants from the test chamber. The tubing and chamber were heated to  $\sim 423 \text{ K}$  ( $150 \text{ }^\circ\text{C}$ ), while purified  $N_2$  flowed through the test setup. After the chamber reached temperature, it was evacuated to  $\sim 3 \text{ Pa}$  using a roughing pump, and then backfilled with purified  $N_2$  three times to rinse the chamber. After the third rinse, the chamber was left to cool to room temperature for more than 12 hours, while purified  $N_2$  continued to flow through the test setup, after which fatigue testing was conducted. Based on previous investigations,<sup>[14]</sup> it was estimated that the gas entering the chamber contained less than 50 ppb of moisture.

As specified in the ASTM Standard E647,<sup>[12]</sup> fatigue-crack growth rates ( $da/dN$ ) were recorded as a function of applied stress intensity range ( $\Delta K = K_{\max} - K_{\min}$ ), where  $K_{\min}$  and  $K_{\max}$  are the minimum and maximum stress intensities sustained by the sample during the

loading cycle. All samples were pre-cracked at  $\Delta K \approx 4$  to 8 MPa $\sqrt{\text{m}}$ . To obtain the fatigue-crack growth curve in air, six samples were used. Three samples were tested under decreasing  $\Delta K$  conditions. Using initial stress intensity ranges of  $\Delta K = 5.8, 3.8,$  and  $3.0$  MPa $\sqrt{\text{m}}$ , the loads were slowly decreased using a constant  $\Delta K$  gradient ( $d\Delta K/da \Delta K^{-1} = -0.08/\text{mm}$ ), which permitted the measurement of a wide range of mid to low growth rates as well as the fatigue threshold,  $\Delta K_{\text{TH}}$ , which was defined as the  $\Delta K$  for which the growth rate was  $<10^{-10}$  m/cycle. For each decreasing  $\Delta K$  test, data collection began after the crack had progressed outside of the calculated (maximum) plane-strain plastic zone formed at  $K_{\text{max}}$  during pre-cracking to avoid transient effects. Additionally, three samples were fatigue cracked with a constant load range ( $\Delta P = 164, 194,$  and  $219$  N) using initial values of  $\Delta K = 3.5, 4.5,$  and  $9.0$  MPa $\sqrt{\text{m}}$ , respectively, to determine higher fatigue-crack growth rates. A strain gage was affixed to the back surface of each sample and used to monitor crack length

progression in the specimen using standard calibrations for the C(T) geometry.<sup>[15]</sup> Actual crack lengths were verified after each test using optical and scanning electron microscopy (Quanta 600F, FEI, Hillsboro, OR).

For the fatigue-crack growth curves in inert (flowing dry gaseous  $\text{N}_2$ ) environment, two samples were tested: One sample was cycled under decreasing load  $\Delta K$  conditions with an initial value of  $\Delta K = 4.0$  MPa $\sqrt{\text{m}}$ , whereas the second was cycled at a constant  $\Delta P$  of 177 N using an initial  $\Delta K$  value of  $3.5$  MPa $\sqrt{\text{m}}$ . All other procedures were identical to those described above for fatigue testing in ambient air.

### III. RESULTS

Fatigue life results for the  $\text{Zr}_{52.5}\text{Cu}_{17.9}\text{Ni}_{14.6}\text{Al}_{10}\text{Ti}_5$  BMG (Vitreloy 105) are shown in Figure 2 in the form of stress–life ( $S/N$ ) curves where the number of cycles to failure,  $N_f$ , is plotted as a function of the stress amplitude normalized by the ultimate tensile strength,  $\sigma_a/\sigma_{\text{UTS}}$ . For comparison, results are also shown from published studies on BMGs with composition  $\text{Zr}_{41.25}\text{Ti}_{13.75}\text{Ni}_{10}\text{Cu}_{12.5}\text{Be}_{22.5}$  (Vitreloy 1).<sup>[4,16]</sup> The  $S-N$  data show a normalized  $10^7$ -cycle endurance strength for Vitreloy 105 of  $\sigma_{\text{fat}}/\sigma_{\text{UTS}} \sim 0.24$ , with an absolute value of  $\sigma_{\text{fat}} = 408$  MPa. Fracture surfaces of selected samples were examined using a Hitachi S-4300SE/N scanning electron microscope to discern the origins and mechanisms of failure, as shown in Figure 3. A majority of the samples failed at their fatigue strength, shown in Figure 2, after cracks initiated close to the tensile surface (Figure 3(a)). Samples containing small amounts of casting porosity (Figure 3(b)), however, displayed a much reduced endurance strength, by as much as  $\sim 60$  pct; those data are not plotted in Figure 2.

Fatigue-crack growth rate ( $da/dN$ ) behavior for Vitreloy 105 was measured in air and dry  $\text{N}_2$  gas and is plotted as a function of the applied stress intensity range ( $\Delta K$ ) in Figure 4. Both fatigue-crack growth curves have three distinct regimes, detailed in Figure 4. Region I in Figure 4 is a discernible low-growth-rate threshold regime where the growth rates are highly sensitive to changes in  $\Delta K$ ; threshold  $\Delta K_{\text{TH}}$  values were

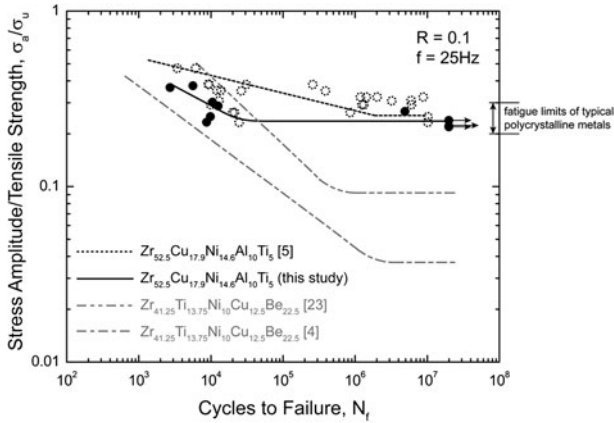


Fig. 2—Stress–life ( $S-N$ ) data for the  $\text{Zr}_{52.5}\text{Cu}_{17.9}\text{Ni}_{14.6}\text{Al}_{10}\text{Ti}_5$  BMG tested at a frequency of 25 Hz (sine wave) and a constant load ratio of  $R = 0.1$  in ambient air. Data are presented in comparison with  $\text{Zr}_{41.25}\text{Ti}_{13.75}\text{Ni}_{10}\text{Cu}_{12.5}\text{Be}_{22.5}$  Vitreloy 1<sup>[4,16]</sup> as well as early  $S-N$  data of  $\text{Zr}_{52.5}\text{Cu}_{17.9}\text{Ni}_{14.6}\text{Al}_{10}\text{Ti}_5$  Vitreloy 105.<sup>[5]</sup> Note in Ref. [16], testing was done in three-point bending, while the rest of the data were collected using four-point bending.

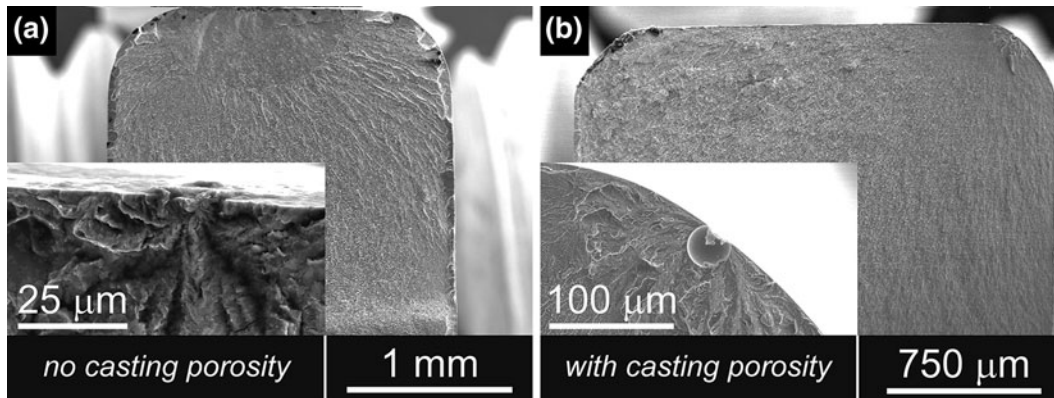


Fig. 3—Micrographs of  $S-N$  samples of  $\text{Zr}_{52.5}\text{Cu}_{17.9}\text{Ni}_{14.6}\text{Al}_{10}\text{Ti}_5$  BMG. (a) Sample without casting porosity showing crack initiation at the tensile surface. (b) Casting porosity leading to failure at a fatigue strength reduced by as much as  $\sim 60$  pct.



found to be  $\sim 2 \text{ MPa}\sqrt{\text{m}}$  and were unchanged in air vs nitrogen gas. Region II shows a distinct intermediate-growth-rate regime in which crack growth increases with increasing  $\Delta K$  according to the Paris law. The medium growth rates for Region II were fit to the classical Paris Law using units of  $m/\text{cycle}$  for  $da/dN$  and  $\text{MPa}\sqrt{\text{m}}$  for  $\Delta K$ <sup>[17]</sup>.

$$\frac{da}{dN} = C\Delta K^m. \quad [2]$$

$C$  and  $m$  were found to be  $\sim 1.35 \times 10^{-10} \text{ MPa}^{-2} \text{ cycle}^{-1}$  and  $\sim 2.0$ , respectively, for Vitreloy 105 in both air and dry  $\text{N}_2$ . Region III is the high-growth-rate region where  $K_{\text{max}}$  approaches the fracture toughness of the material prior to final failure.

#### IV. DISCUSSION

Many factors can affect the measured fatigue life properties in bending including sample preparation (*e.g.*, polishing, porosity, *etc.*) and bending configuration (*e.g.*, inner loading span). As such, a large range of endurance limits has been reported (Figure 2) for the most studied BMG composition  $\text{Zr}_{41.25}\text{Ti}_{13.75}\text{Ni}_{10}\text{Cu}_{12.5}\text{Be}_{22.5}$  (Vitreloy 1). However, it can also be seen in Figure 2 that this range of reported behavior is not sufficiently wide to include fatigue resistance anywhere near the excellent properties of  $\text{Zr}_{52.5}\text{Cu}_{17.9}\text{Ni}_{14.6}\text{Al}_{10}\text{Ti}_5$  (Vitreloy 105) reported here and elsewhere.<sup>[5]</sup> To explain this discrepancy, other factors must be considered such as the role of the environment.

Fatigue-crack growth rate data collected for Vitreloy 105 are compared in Figure 5 to results taken from References 7 and 10 for a  $\text{Zr}_{44}\text{Ti}_{11}\text{Ni}_{10}\text{Cu}_{10}\text{Be}_{25}$  BMG (Vitreloy 1b) tested in inert dry  $\text{N}_2$  environment (Figure 5(a)) and in ambient air (Figure 5(b)). It is apparent that for ambient air, the Vitreloy 1b data display a fourth growth region near  $10^{-9} \text{ m/cycle}$  which is stress intensity independent (Figure 5(b)). In the mid-range of growth rates, however,  $C$  was reported to be  $1.8 \times 10^{-10} \text{ MPa}^{-2} \text{ cycle}^{-1}$  and with an exponent  $m$  of  $\sim 2.0$  in air,<sup>[10]</sup> whereas for dry  $\text{N}_2$ , the corresponding values were  $C = 8.5 \times 10^{-11} \text{ MPa}^{-2} \text{ cycle}^{-1}$  and  $m \sim 2.3$ <sup>[7]</sup>; values of the fatigue threshold  $\Delta K_{\text{TH}}$  were  $< 1.5 \text{ MPa}\sqrt{\text{m}}$  in laboratory air and  $\sim 2 \text{ MPa}\sqrt{\text{m}}$  in the inert environment (Figure 5).

Vitreloy 1b clearly shows a degradation of the fatigue behavior in air with a much lower fatigue threshold. In contrast, the present Vitreloy 105 glass can be seen to exhibit similar fatigue behavior in both inert and ambient room air ( $\sim 20$  to 40 pct relative humidity), with a fatigue threshold  $\Delta K_{\text{TH}}$  comparable to that of Vitreloy 1b tested in inert environment. Furthermore, unlike most Zr-based BMGs which have been tested in air, including  $\text{Zr}_{41.25}\text{Ti}_{13.75}\text{Ni}_{10}\text{Cu}_{12.5}\text{Be}_{22.5}$  (Vitreloy 1),  $\text{Zr}_{44}\text{Ti}_{11}\text{Ni}_{10}\text{Cu}_{10}\text{Be}_{25}$  (Vitreloy 1b), and  $\text{Zr}_{58.5}\text{Cu}_{15.6}\text{Ni}_{12.8}\text{Al}_{10.3}\text{Nb}_{2.8}$  (Vitreloy 106a),<sup>[8–11]</sup> a fatigue-crack growth plateau is not seen for the Vitreloy 105 glass. Mechanistically, a stress intensity-insensitive plateau in the fatigue-crack growth rate vs stress intensity curve invariably implies that

something other than mechanically induced damage is acting as the rate-limiting step in the crack growth process; this is commonly associated with an environment interaction such as a rate-limiting step involving the oxidation of the freshly exposed surface at the crack tip or the transport of the active environmental species to, or ahead of, this crack tip.<sup>[18,19]</sup> This is apparent for Vitreloy 1b as the plateau does not occur in the samples tested in inert dry  $\text{N}_2$  gas.<sup>[7]</sup> Fatigue and sustained load cracking behavior in Vitreloy 1 is also known to be highly sensitive to environmental effects in aqueous environments.<sup>[20]</sup>

The current study provides clear evidence that the composition  $\text{Zr}_{52.5}\text{Cu}_{17.9}\text{Ni}_{14.6}\text{Al}_{10}\text{Ti}_5$  (Vitreloy 105) has little such susceptibility to environmental effects in ambient air, with a fatigue threshold that is essentially identical in air and inert atmosphere. Furthermore, the measured fatigue threshold of  $\sim 2.0 \text{ MPa}\sqrt{\text{m}}$  is higher than values reported for residual stress-relieved samples made from other Zr-based BMGs tested in air such as Vitreloy 1b (Figure 5(b)) and Vitreloy 106a ( $\Delta K_{\text{TH}} < 1.4 \text{ MPa}\sqrt{\text{m}}$ ).<sup>[10,11]</sup>

Due to the absence of an environmental effect on fatigue-crack growth, Vitreloy 105 exhibits considerably higher overall fatigue resistance than other Zr-based metallic glasses. In addition to the relatively high fatigue threshold of  $\sim 2 \text{ MPa}\sqrt{\text{m}}$ , the strength-normalized endurance limit is  $\sigma_{\text{fat}}/\sigma_{\text{UTS}} \approx 0.24$  (four-point bending,  $R = 0.1$ ) as seen in Figure 2 and References 5 and 6. These key fatigue properties are comparable to, or better than, many crystalline metallic alloys.

These favorable fatigue properties, along with other attractive BMG attributes such as high strength ( $\sim 1700 \text{ MPa}$ <sup>[5,21]</sup>), a relatively high reported fracture toughness of  $49 \text{ MPa}\sqrt{\text{m}}$ ,<sup>[22]</sup> a critical cooling rate as low as  $10 \text{ K/s}$ ,<sup>[13]</sup> and the fact that it does not contain beryllium, make the  $\text{Zr}_{52.5}\text{Cu}_{17.9}\text{Ni}_{14.6}\text{Al}_{10}\text{Ti}_5$  Vitreloy 105 BMG a particularly attractive candidate for use in mechanical components. However, proper processing is essential to avoid porosity that can drastically reduce

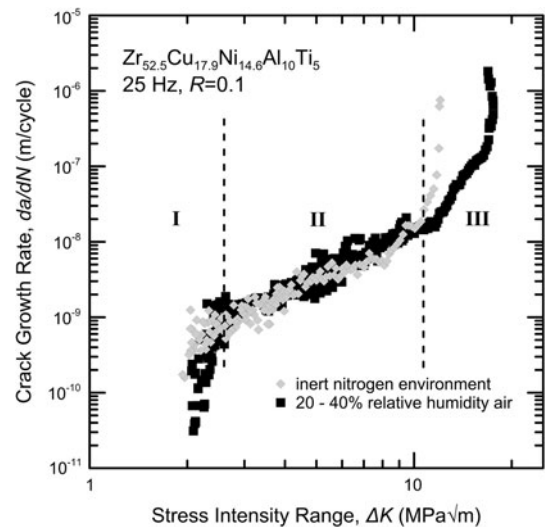


Fig. 4—Comparison of fatigue-crack growth rate data for the  $\text{Zr}_{52.5}\text{Cu}_{17.9}\text{Ni}_{14.6}\text{Al}_{10}\text{Ti}_5$  BMG collected in 20 to 40 pct relative humidity air and in inert dry  $\text{N}_2$  environment.

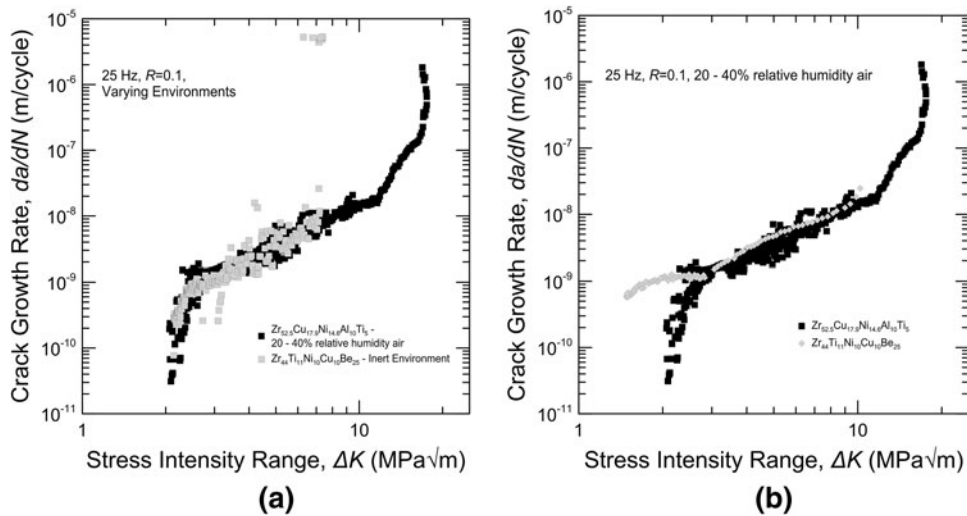


Fig. 5—Fatigue-crack growth rate data for the  $Zr_{52.5}Cu_{17.9}Ni_{14.6}Al_{10}Ti_5$  BMG tested in air are compared to (a)  $Zr_{44}Ti_{11}Ni_{10}Cu_{10}Be_{25}$  tested in inert dry  $N_2$  environment<sup>[7]</sup> and (b)  $Zr_{44}Ti_{11}Ni_{10}Cu_{10}Be_{25}$  tested in air.<sup>[10]</sup>

the fatigue life. Also, it should not be assumed this BMG would be appropriate for use in all environments; indeed, one study showed a drastic 88 pct decrease in the endurance limit in 0.6 M NaCl aqueous solution.<sup>[23]</sup>

Finally, it is interesting to note that BMG matrix composites also demonstrate a wide range of fatigue behavior with  $\sigma_{fat}/\sigma_{UTS}$  ranging between 0.07 and 0.30 for various Zr-based BMG matrix composites.<sup>[24–26]</sup> Like with monolithic BMGs, the behavior can range from very poor to excellent, further reinforcing the notion that the presence of a microstructure is not the key to high fatigue strength. In the case of the composite with the lowest fatigue resistance,<sup>[24]</sup> the BMG matrix is of the composition Zr-Ti-Ni-Cu-Be. Thus, the matrix composition is similar to the monolithic Vitreloy 1 and 1b BMGs which are known to have poor fatigue resistance attributed to the ambient air environment.<sup>[7]</sup> Accordingly, it is likely that the composites with good fatigue resistance have BMG matrix compositions that are less affected by ambient air environments. This is an area for future investigations.

## V. CONCLUSIONS

Based on an experimental study of the fatigue life and fatigue-crack growth behavior of a  $Zr_{52.5}Cu_{17.9}Ni_{14.6}Al_{10}Ti_5$  BMG (Vitreloy 105), the following conclusions can be made.

- The excellent reported fatigue life behavior of Vitreloy 105 was confirmed with a measured ratio of  $2 \times 10^7$  cycle fatigue endurance strength to the ultimate tensile strength of  $\sim 0.24$  ( $R = 0.1$ ). This is as high as any BMG reported to date and comparable to most crystalline structural metals and alloys. However, it was also found that small amounts of casting porosity can reduce the fatigue endurance strength by as much as  $\sim 60$  pct.

- The excellent fatigue life behavior was attributed to a relatively high fatigue threshold ( $\Delta K_{TH} \approx 2 \text{ MPa}\sqrt{\text{m}}$ ) and a relative insensitivity to environmental degradation which is known to accelerate fatigue-crack growth rates in ambient air for other Zr-based BMGs. Indeed, unlike other Zr-based BMGs tested in ambient air, Vitreloy 105 did not exhibit a regime where crack growth was independent of the applied stress intensity and the behavior in room air was identical to that in inert environment. The results of this study indicate that a key part of engineering fatigue resistance into BMGs is choosing the correct chemistry to avoid detrimental environmental effects on cracking behavior.
- Overall, Vitreloy 105 appears to have excellent strength and fatigue properties and should be considered as a prime candidate for future use in mechanical components that require fatigue resistance. These qualities support the possibility that BMGs could be used in industries where lightweight and fatigue-resistant structural materials are needed to improve performance and energy efficiency.

## ACKNOWLEDGMENTS

The authors wish to thank Melissa McGee for aid in sample preparation and testing and Andy Waniuk of Liquidmetal Technologies for help in preparing the BMG plates. Support for BG and ROR was provided by the Director, Office of Science, Office of Basic Energy Sciences, Division of Materials Sciences and Engineering, of the U.S. Department of Energy under Contract No. DE-AC02-05CH11231. JJK would like to acknowledge the support of the Arthur E. Hitsman Faculty Scholarship.

## REFERENCES

1. C.J. Byrne and M. Eldrup: *Science*, 2008, vol. 321, pp. 502–03.
2. M.F. Ashby and A.L. Greer: *Scripta Mater.*, 2006, vol. 54, pp. 321–26.
3. J. Schroers: *JOM*, 2005, vol. 57, pp. 35–39.
4. C.J. Gilbert, J.M. Lippmann, and R.O. Ritchie: *Scripta Mater.*, 1998, vol. 38, pp. 537–42.
5. M.L. Morrison, R.A. Buchanan, P.K. Liaw, B.A. Green, G.Y. Wang, C. Liu, and J.A. Horton: *Mater. Sci. Eng. A*, 2007, vol. 467, pp. 190–97.
6. G.Y. Wang, P.K. Liaw, and M.L. Morrison: *Intermetallics*, 2009, vol. 17, pp. 579–90.
7. S.L. Philo and J.J. Kruzic: *Scripta Mater.*, 2010, vol. 62, pp. 473–76.
8. J.J. Kruzic: *Metall. Mater. Trans. A*, 2011, vol. 42A, pp. 1516–23.
9. C.J. Gilbert, V. Schroeder, and R.O. Ritchie: *Metall. Mater. Trans. A*, 1999, vol. 30A, pp. 1739–53.
10. M.E. Launey, R. Busch, and J.J. Kruzic: *Acta Mater.*, 2008, vol. 56, pp. 500–10.
11. S.L. Philo, J. Heinrich, I. Gallino, R. Busch, and J.J. Kruzic: *Scripta Mater.*, 2011, vol. 64, pp. 359–62.
12. ASTM Standard E647, 2008e1: *Standard Test Method for Measurement of Fatigue Crack Growth Rates*, ASTM International, West Conshohocken, PA, U.S.A., 2008, DOI: [10.1520/E0647-08E01](https://doi.org/10.1520/E0647-08E01), <http://www.astm.org>.
13. X.H. Lin, W.L. Johnson, and W.K. Rhim: *Mater. Trans. JIM*, 1997, vol. 38, pp. 473–77.
14. J.J. Kruzic, R.M. Cannon, and R.O. Ritchie: *J. Am. Ceram. Soc.*, 2005, vol. 88, pp. 2236–45.
15. D.C. Maxwell: Report No. AFWAL-TR-87-4046, Air Force Wright Aeronautical Laboratories, 1987.
16. M.E. Launey, R. Busch, and J.J. Kruzic: *Scripta Mater.*, 2006, vol. 54, pp. 483–87.
17. P.C. Paris, M.P. Gomez, and W.P. Anderson: *Trend Eng.*, 1961, vol. 13, pp. 9–14.
18. A.J. McEvily and R.P. Wei: in *Corrosion Fatigue: Chemistry, Mechanics and Microstructure*, O. Devereux, A.J. McEvily, and R.W. Staehle, eds., National Association of Corrosion Engineers, Houston, TX/Storrs, CT, 1972, pp. 381–95.
19. S. Suresh: *Fatigue of Materials*, 2nd ed., Cambridge University Press, Cambridge, 1998.
20. V. Schroeder and R.O. Ritchie: *Acta Mater.*, 2006, vol. 54, pp. 1785–94.
21. C.T. Liu, L. Heatherly, D.S. Easton, C.A. Carmichael, J.H. Schneibel, C.H. Chen, J.L. Wright, M.H. Yoo, J.A. Horton, and A. Inoue: *Metall. Mater. Trans. A*, 1998, vol. 29A, pp. 1811–20.
22. J.H. Schneibel, J.A. Horton, and P.R. Munroe: *Metall. Mater. Trans. A*, 2001, vol. 32A, pp. 2819–25.
23. M.L. Morrison, R.A. Buchanan, P.K. Liaw, B.A. Green, G.Y. Wang, C.T. Liu, and J.A. Horton: *Mater. Sci. Eng. A*, 2007, vol. 467A, pp. 198–206.
24. K.M. Flores, W.L. Johnson, and R.H. Dauskardt: *Scripta Mater.*, 2003, vol. 49, pp. 1181–87.
25. M.E. Launey, D.C. Hofmann, W.L. Johnson, and R.O. Ritchie: *Proc. Natl. Acad. Sci. U.S.A.*, 2009, vol. 106, pp. 4986–91.
26. J.W. Qiao, E.W. Huang, G.Y. Wang, H.J. Yang, W. Liang, Y. Zhang, and P.K. Liaw: *Mater. Sci. Eng. A*, 2013, vol. 563, pp. 101–05.